JOURNAL OF MATERIALS SCIENCE **40** (2005) 2341 – 2348

Interfacial analysis of $(La_{0.6}Sr_{0.4})(Co_{0.2}Fe_{0.8})O_{3-\delta}$ substrates wetted by Ag-CuO

K. SCOTT WEIL*, JIN YONG KIM, JOHN S. HARDY
Pacific Northwest National Laboratory, P.O. Box 999, Richland, WA 99352, USA
E-mail: scott.weil@pnl.gov

The wetting of $(La_{0.6}Sr_{0.4})(Co_{0.2}Fe_{0.8})O_{3-\delta}$ substrates by Ag-CuO was investigated using the standard sessile drop technique, followed by metallographic examination of the quenched specimens. The addition of CuO substantially improves the wetting of these substrates by silver. The largest improvements in contact angle are observed at low CuO-content, apparently through the formation of a homogeneous silver-copper oxide liquid at the area of sessile drop/substrate contact. At a critical composition of $x_{CuO} \sim 8$ mol% the mechanism of wetting changes, undergoing a transition initiated by the formation of two immiscible liquids within the molten sessile drop.

1. Introduction

The development of high-temperature electrochemical devices such as oxygen and hydrogen separators, fuel gas reformers, and chemical sensors is part of a rapidly expanding segment of the solid-state technology market [1]. These devices employ a mixed ionic/electronic conducting oxide (MCO) as an active membrane that facilitates ionic transport, e.g. O^{-2}, at high temperature when placed under an appropriate chemical gradient. Because device performance is proportional to the magnitude of this gradient, hermiticity across the MCO is paramount. That is, not only must this thin ceramic membrane be dense with no interconnected porosity, but it must be connected to the rest of the device with a high-temperature, gas-tight seal. Therein lies one of the key issues in fabricating these types of devices; effecting a seal that remains hermetic, rugged, and stable under continuous high temperature operation. A particular challenge is in sealing directly to the MCO. Both the transport and mechanical properties of the perovskite oxides typically employed in their membranes are sensitive to: (1) oxygen partial pressure [2] (i.e. they tend to irreversibly degrade under the high temperature vacuum conditions typically employed in traditional ceramic brazing) and (2) A- and B-site cation substitution [3]. Thus the compatibility of the joining material with respect to both conditions must be carefully considered.

In the past couple of years several groups have independently developed a new ceramic brazing technique, referred to as air brazing, that forms a predominantly metallic joint directly in air without need of an inert cover gas or use of surface reactive fluxes [4–6]. The process employs a braze composition that when molten consists of a metal oxide dissolved in a noble metal filler. Potential air braze systems include Pt-Nb_2O_3, Ag-CuO, and Ag-V_2O_5 [7]. To date much of the work reported on air brazing has concentrated on the latter two systems. For example, Schüler *et al.* were the first to discuss the use of Ag-1% CuO in bonding alumina for electronic applications [4], while Erskine *et al.* have examined the joining of piezoelectric niobates with Ag-V_2O_5 for use in acoustic sensors [5]. In our work, we have developed air brazing as a means of hermetically sealing solid-state electrochemical devices such as solid oxide fuel cells and gas concentrators [6]. While much of this effort has focused on the feasibility of air brazing, little emphasis has been placed on understanding the wetting characteristics of the various filler material systems as a function of braze or substrate composition.

The goal of the present study is to systematically investigate the compositional dependence of the contact angle formed between Ag-CuO based brazes and a prototypical oxygen transport material. Lanthanum strontium cobalt ferrite, $(La_{0.6}Sr_{0.4})(Co_{0.2}Fe_{0.8})O_{3-\delta}$ (LSCoF), was chosen as the MCO for study. Because of its substituted nature, the compound displays excellent ionic and electronic transport properties, which make it a strong candidate for use in commercial oxygen generators [8]. However, it is particularly sensitive to oxygen partial pressure at high temperature and will experience oxygen loss and eventual phase separation under low p_{O_2} environments [8]. Thus while active metal brazing cannot be used to join this material, air brazing is potentially a viable sealing technique. As will be discussed, wetting in the Ag-CuO air braze system occurs via one of two mechanisms that depend on the miscible nature of the liquid phases that form within the braze during melting.

2. Experimental procedure

Contact angles were measured in an air muffle furnace using the classical sessile drop technique [9]. Polished, high density LSCoF tablets were employed as the

*Author to whom all correspondence should be addressed.

wetting substrates. Sintered Ag-CuO pellets were heated on these substrates to the molten state and the shape of the resulting drop was recorded as a function of time and temperature using a high speed video camera. After quenching to room temperature, the wetting specimens were mounted, cut, and polished for characterization by scanning electron microscopy (SEM) and energy dispersive X-ray analysis (EDX).

2.1. Materials

High purity LSCoF powder (99.9% purity; Praxair Specialty Ceramics, Inc.) was uniaxially compacted into 12 mm × 20 mm tablets using a hydraulic press. The tablets were further densified under 20 ksi of isostatic pressure and sintered in air at 1250°C for two hours. With an average density of 96% of theoretical, the as-sintered substrates measured approximately 10 mm × 17 mm × 3 mm thick. The wetting surface of each pellet substrate was polished with diamond paste using successively finer grit, with 0.1 μm grit used in the final step. On average, the surface roughness was 4 nm with a maximum height of 21 nm, as measured by a profilometer. Prior to performing the wetting experiments, the polished surfaces were cleaned with acetone, rinsed with propanol, air dried, and heated in static air to 600°C for four hours to burn off any residual organic contamination.

Braze compositions were prepared in the form of pressed pellets. These were fabricated by dry mixing copper (99% purity; 1.4 μm average particle size; Alfa Aesar) and silver (99.9% purity; 0.7 μm average particle size; Alfa Aesar) powders in the ratios required to yield the target compositions listed in Table I. These compositions assume that the copper is completely oxidized prior to use. To ensure this and promote homogeneous dispersion of the oxide, the powder mixtures were first uniaxially pressed into pellets measuring 0.6 mm in diameter by ∼0.6 mm thick. Then based on X-ray diffraction and metallographic results obtained from a prior series of heat treatment experiments, the pellets were pre-treated in air at 700°C for 4 h to completely oxidize the copper to CuO and to facilitate homogenization of this species within the pellet. The pellet densities averaged ∼65% of the theoretical density as determined by geometric measurement and rule of mixtures calculations.

TABLE I Target compositions of the Ag-CuO filler materials investigated in this study

Braze ID	Ag content (mol%)	CuO content (mol%)
CA0	100	0
CA01	99	1
CA01.4	98.6	1.4
CA02	98	2
CA04	96	4
CA08	92	8
CA16	84	16
CA34	66	34
CA69	30.7	69.3

2.2. Characterization techniques

The sessile drop experiments were conducted by placing a braze pellet on the polished surface of a LSCoF substrate, heating both to a temperature at which the pellet becomes molten, and monitoring the variation in the braze droplet's base diameter, height, and angle of contact it forms with the substrate during a series of isothermal soaks. The experiments were carried out in a static air box furnace equipped with a transparent quartz window on the front door through which the heated specimen could be observed. A high speed video camera fitted with a 50× zoom lens was used to record changes in the wetting specimen over the entire heating cycle. The specimens initially were heated quickly at 30°C/min to a sub-liquidus temperature of 900°C, at which point the heating rate was reduced to10°C/min for the rest of the cycle. Once stable at 900°C, the furnace temperature was then raised to 950°C, where the temperature remained for fifteen minutes, increased again to a second isothermal hold at 1000°C for fifteen minutes, followed by a third fifteen minute soak at 1050°C, and subsequently heated to a final fifteen minute dwell at 1100°C. In this way, the shape of the sessile drop was allowed to stabilize for measurement at each temperature. Once the wetting experiment concluded, each sample was quenched at 10°C/min to 550°C, then furnace cooled to room temperature.

Conversion of the analog video data to digital form for image analysis was performed using VideoStudio6™ (Ulead Systems, Inc.) frame capturing and video editing software. The digitalized images were subsequently imported into Canvas™ graphic software (version 8.0.5, Deneba Systems, Inc.) for droplet shape measurement. The outline of the droplet was circumscribed with a circle of best fit, which was used to determine the droplet's radius. The contact angle was then calculated from the radius and the diameter of contact between the droplet and the substrate. Microstructural analysis was conducted on polished cross-sectioned samples by SEM (JEOL JSM-5900LV) and EDX (Oxford Systems). The SEM is equipped with a windowless detector, allowing detection and quantitative measurement of both light and heavy elements. To avoid electrical charging of the samples in the SEM, they were carbon coated and grounded. Elemental profiles were recorded across joint interfaces in the line-scan mode.

3. Results

3.1. Contact angle measurements

Shown in Fig. 1a and b are the contact angles measured between molten Ag-CuO and LSCoF as a function of copper oxide content and temperature. During the initial stage of heating each composition, liquefaction was observed to begin approximately at the temperature predicted by the Ag-CuO phase diagram [10], implying that neither diffusion nor solid-state reaction kinetics significantly impeded the CuO and Ag from reaching equilibrium. In addition, the fifteen minute isothermal

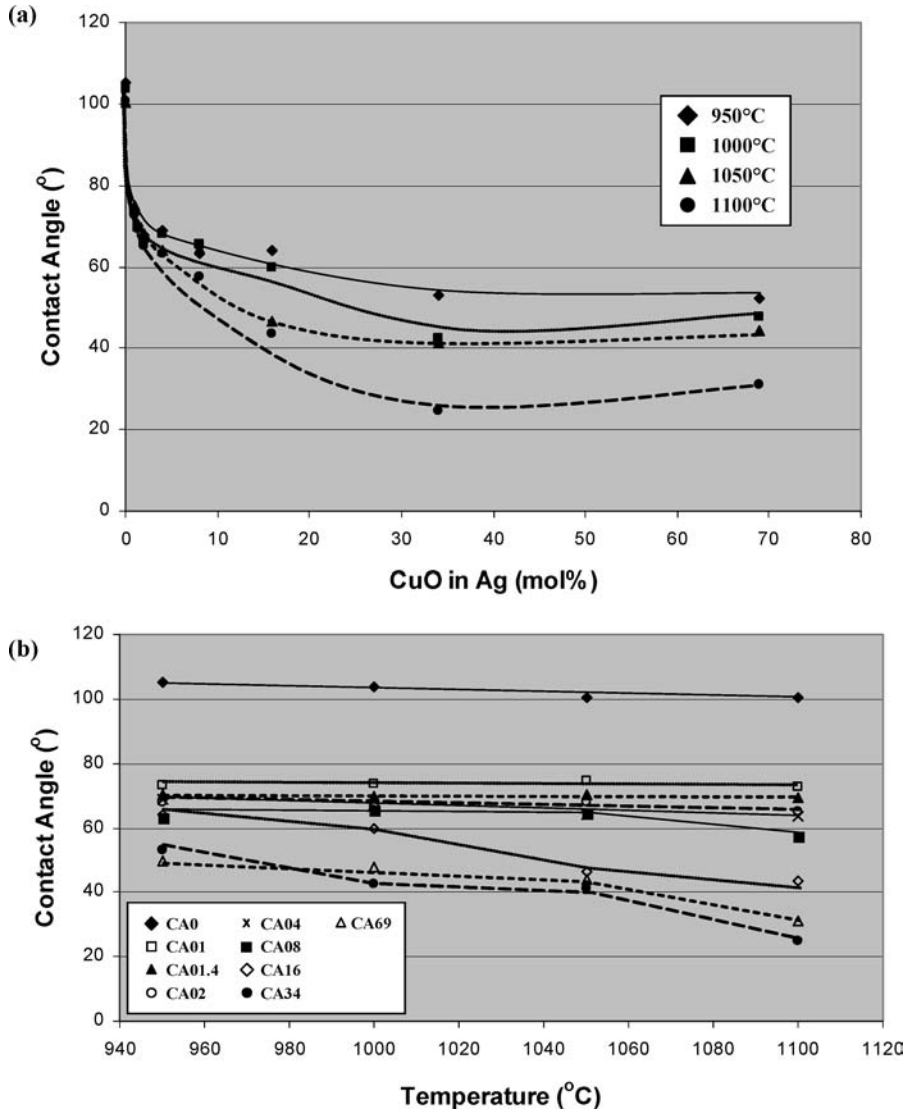

Figure 1 A plot of the contact angle formed between Ag-CuO and LSCoF as a function of: (a) CuO content and (b) temperature.

dwell times employed in the heating cycle appeared to be sufficiently long for the contact angles to reach their equilibrium values.

As seen in Fig. 1a, independent of temperature the addition of CuO causes a significant decrease in the contact angle between the molten drop and LSCoF, from the non-wetting condition displayed by pure silver to an apparent minimum value reached at ∼35 mol% CuO. Much of the drop occurs in a narrow compositional band bounded at an upper limit of $X_{\mathrm{CuO}} \approx 4$ mol%. In fact, each curve appears to consist of three distinct regions, as defined by obvious changes in slope: (1) $0 < X_{\mathrm{CuO}} \lesssim 4$ mol%, where the greatest decrease in contact angle occurs; (2) 4 mol% $\lesssim X_{\mathrm{CuO}} \lesssim 35$ mol%, denoted by a more gradual decrease in contact angle as a function of composition; and (3) 35 mol% $\lesssim X_{\mathrm{CuO}} \lesssim 69$ mol%, in which a small, but reproducible increase in contact angle is observed at the end point composition. In Fig. 1b, a second compositional effect on wetting behavior is observed. Below 8 mol% CuO content (specimens CA0 – CA04), the contact angle appears to be nearly invariant of temperature. However at this threshold and above, contact angle decreases with increasing temperature.

3.2. Microstructural analysis

After quenching, metallographic analysis was conducted on the wetting specimens. Typical results for sessile drop compositions of 0–4 mol% CuO in Ag are shown in the back scattered electron images of Fig. 2. In the pure silver specimen (CA0) seen in Fig. 2a, the microstructure at the area of contact between the solidified droplet and the LSCoF is characterized by a clean interface decorated with an occasional large void. Although porosity is evident in both the bulk and surface of the LSCoF pellet (as it is in all of the wetting specimens), the filler metal did not appear to penetrate any of these pores. This behavior correlates directly with the macroscopic, non-wetting contact angle of 101° observed in the specimen at 1100°C.

Shown in Fig. 2b is the interfacial microstructure in specimen CA01.4. At this magnification, the interface was found to be similar in appearance to that of the pure silver specimen, although fewer interfacial voids were observed. In fact, a small amount of filler material appears to have infiltrated some of the surface pores of the substrate, as denoted by the two arrows in the figure. Upon analysis conducted at higher magnification, a number of sub-micron CuO particles were observed

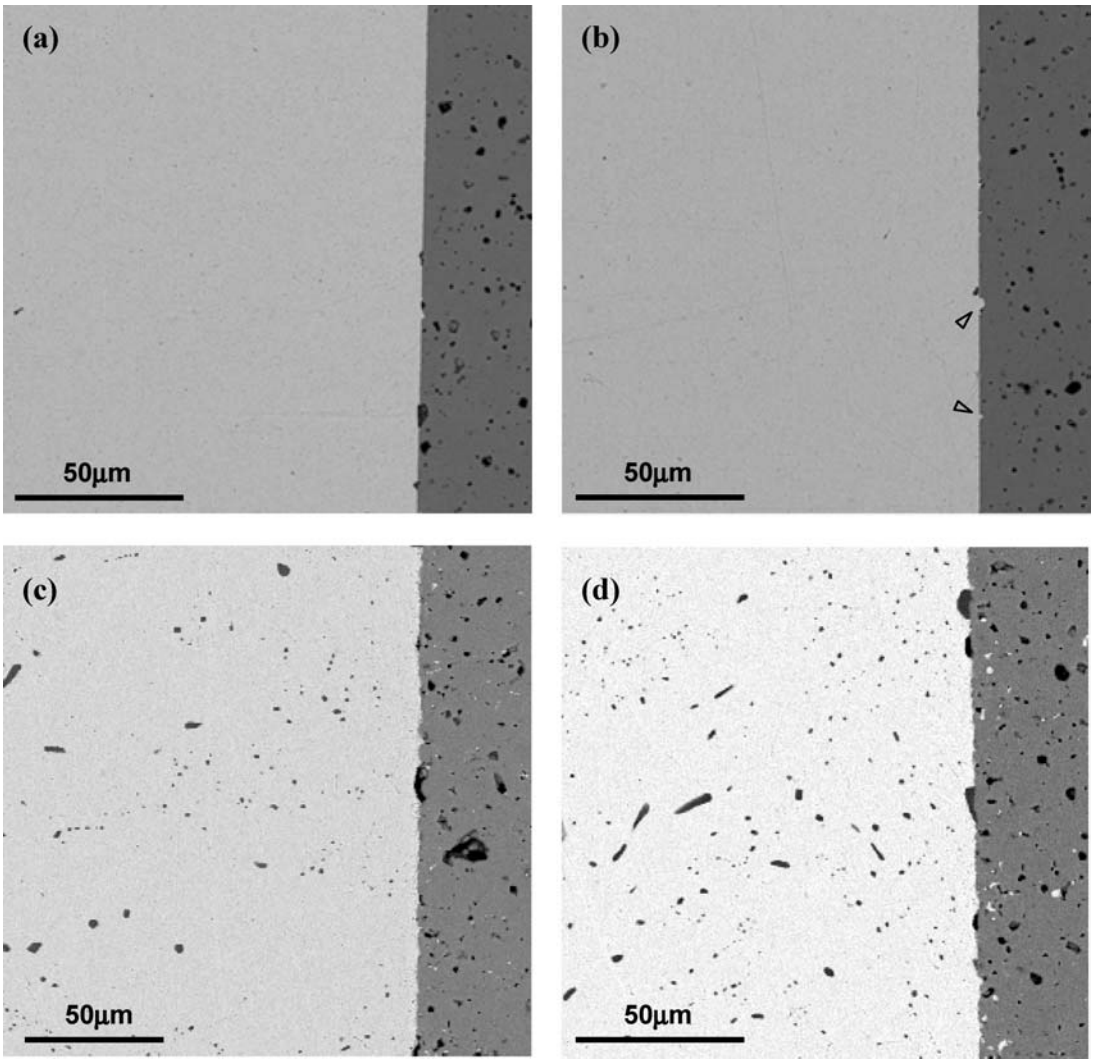

Figure 2 Cross-sectional SEM micrographs of the Ag-CuO sessile drop/LSCoF interface in the following specimens: (a) CA0, (b) CA01.4, (c) CA02, and (d) CA04. The filler material is observed on the left-hand side of each micrograph and the LSCoF substrate is on the right.

both within the silver matrix and along the interface with the LSCoF.

In the specimen wetted by 2 mol% CuO in Ag (CA02), shown in Fig. 2c, the copper oxide is observed to form as larger precipitates both within the filler matrix, which is pure silver, and along the wetting surface of the substrate. In the bulk of the sessile drop, the majority of these particles are spherical in shape and range in size from 3 to 8 μm. A smaller number of these appear to be more elongated in shape and generally larger, on the order of 10–15 μm long. The oxide precipitates at the interface assume a half-lens shaped morphology. In CA04 (Fig. 2d), in which the sessile drop composition is enriched with twice as much CuO, the dispersion of oxide particulate in the matrix is more dense and a larger number of elongated precipitates is observed. The population of precipitates along the sessile drop/substrate interface is also higher and these particles are larger in size than those in CA02. EDX data collected on a large sampling of regions adjacent to the wetting interface in each specimen revealed no indication of a metathetic interfacial reaction between the droplet and the substrate. However, we did observe some infiltration of the filler material into the surface and interconnected sub-surface porosity. The average depth of penetration appears to progress with increasing CuO content in the sessile drop.

Shown in Fig. 3a–d are micrographs of the specimens wetted by the higher CuO-containing braze compositions. In the CA08 specimen shown in Fig. 3a, a nearly continuous 3 μm thick band of CuO is observed in direct contact with the sessile drop/substrate interface. Shown in Figs 3b and c respectively are the microstructures for specimens CA16 and CA34, which are quite similar to each other. The bulk region of each braze droplet is composed primarily of a silver matrix containing a fine-scale dispersion of sub-micron, spherical-shaped copper oxide particles. Very little CuO is observed at the interface with the substrate. Instead, a substantial amount of filler material infiltration has occurred within the interconnected sub-surface porosity. Also observed in these specimens was evidence of an edge effect. Outside the leading edge of the solidified sessile drop, infiltration of the substrate porosity takes place, extending as far as 100 μm ahead of the air-sessile drop-substrate boundary.

The microstructure of CA69 differs completely from those of the previous specimens, as shown in Fig. 3d. The solidified braze droplet is composed primarily of copper oxide. The majority of the silver appears to have

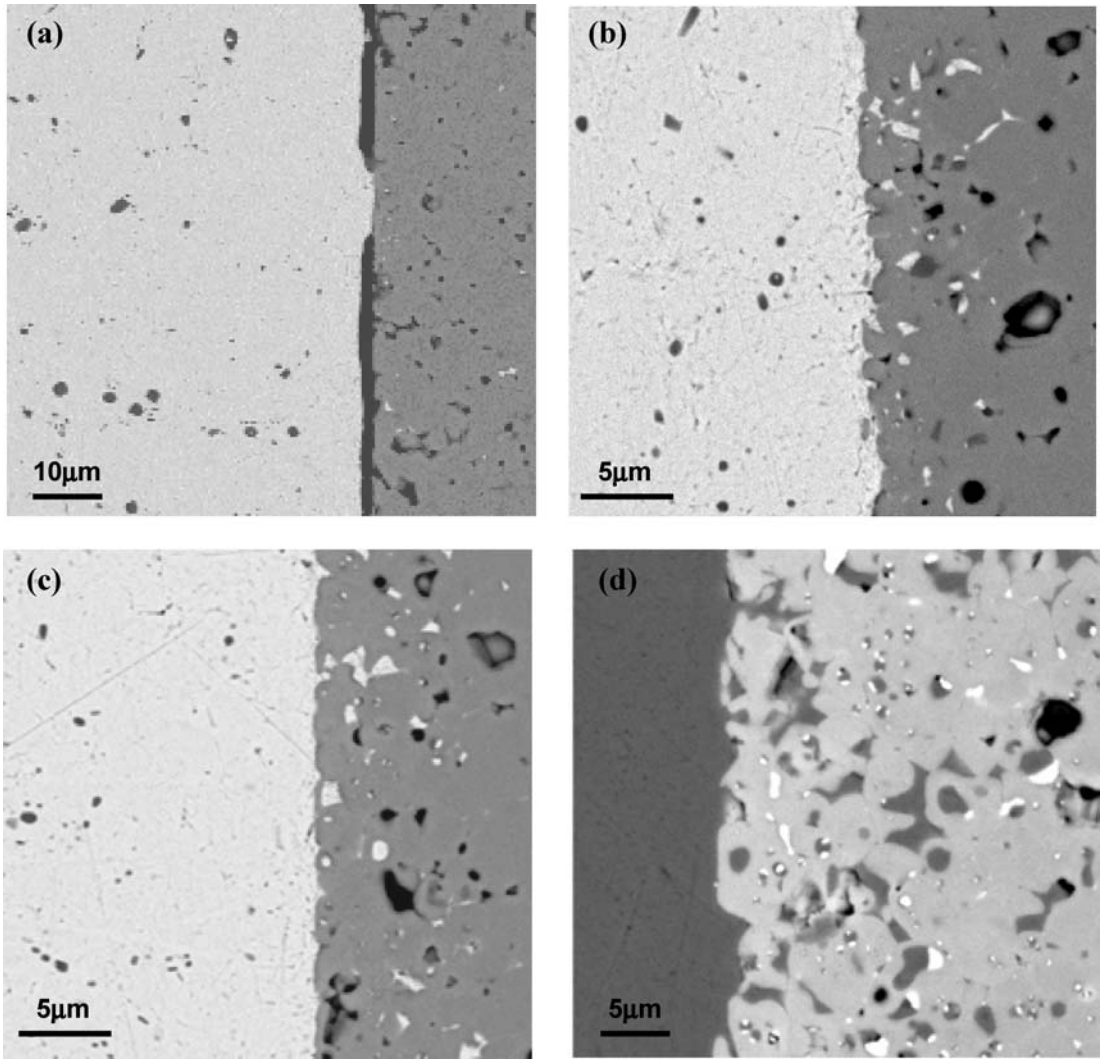

Figure 3 Cross-sectional SEM micrographs of the Ag-CuO sessile drop/LSCoF interface in the following specimens: (a) CA08, (b) CA16, (c) CA34, and (d) CA69. The filler material is observed on the left-hand side of each micrograph and the LSCoF substrate is on the right.

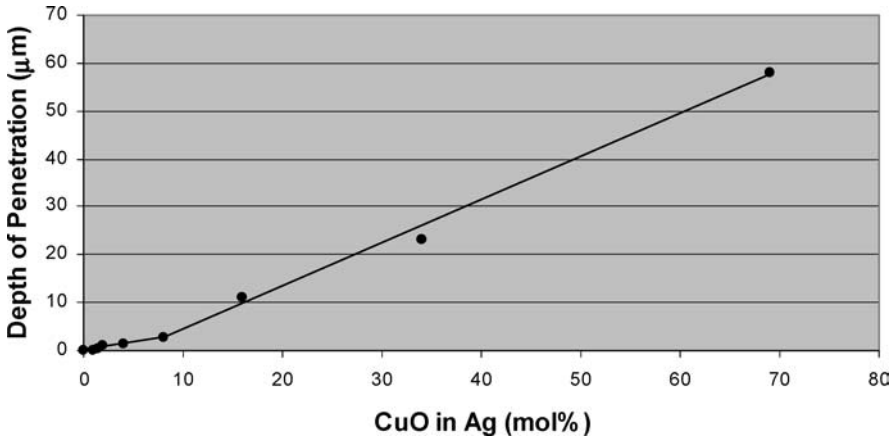

Figure 4 A plot of the depth of filler material penetration into sub-surface substrate porosity as a function of sessile drop composition.

infiltrated far into the underlying substrate through the available interconnected porosity. The average distance of penetration has been tracked EDX and is plotted for all nine specimens in Fig. 4. The depth of penetration correlates directly with CuO content, with an abrupt change in slope observed at a composition of ∼8 mol% CuO in Ag. Again, there was no evidence of a metathetic reaction between the braze material and the substrate, but we did find signs of apparent compositional substitution occurring between the copper oxide and the LSCoF. An example of this is seen in Fig. 5, which shows a high magnification cross-sectional micrograph of the CuO/LSCoF interface in CA08. Corresponding EDX analysis of each labeled region in the image is presented alongside. Approximately 2–5 atom% copper was found in the LSCoF at and adjacent to the interface

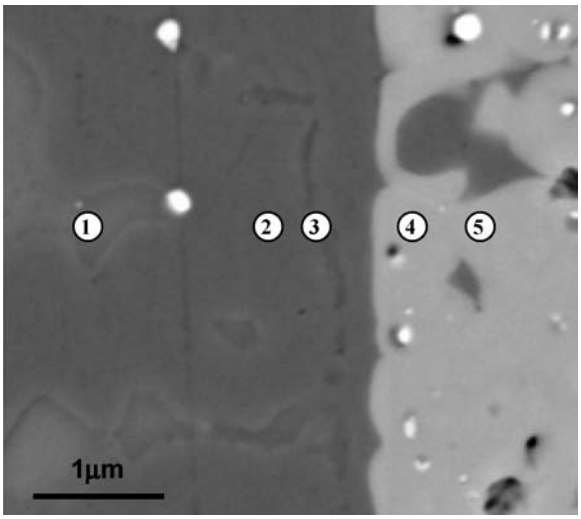

EDX Analysis of Points 1–5

	Composition, at%					
Element	La	Sr	Co	Fe	Cu	Ag
Point 1	1.0	0.9	5.9	2.3	89.9	–
Point 2	–	–	3.7	0.7	86.5	9.1
Point 3	–	–	5.5	2.1	92.4	–
Point 4	26.8	24.1	7.4	36.5	5.2	–
Point 5	26.1	23.0	10.4	37.2	3.3	–

Figure 5 A high magnification cross-sectional SEM micrograph of the sessile drop/substrate interface in CA08. Results from corresponding EDX analysis of the regions labeled in the image are given in the adjacent table.

down to a maximum depth of ∼2 μm. A corresponding amount of cobalt was measured in the CuO band at this interface and appeared to be uniformly mixed throughout, suggesting that a $Cu^{+2} \leftrightarrow Co^{+2}$ exchange reaction occurred when this layer was still molten. Transition metal cation substitution in lanthanum ferrite is well documented and the exchange of copper for cobalt is not surprising [11, 12]. Similarly, molten copper oxide is known to dissolve cobalt oxide and form a solid solution at low alloying additions [13].

4. Discussion

The above results demonstrate that the addition of copper oxide significantly affects the wetting characteristics of silver on LSCoF. As observed previously, distinct regions of wetting behavior are apparent in the contact angle versus composition curves of Fig. 1a. In order to explain this effect, we refer to the Ag-CuO phase diagram of Shao *et al.* [10] shown in Fig. 6. At relatively low CuO-content, a single phase liquid forms at 1100°C. This liquid is rich in silver, but does contain a small amount of CuO, the level of which depends on the original composition of the braze. At a temperature of 1100°C and a composition of ∼8 mol% CuO, the liquid displays immiscibility and while the wetting angle continues to decrease with additional CuO, Fig. 1a, it does so only gradually. At $x_{CuO} > 8$ mol%, two liquids form within the molten sessile drop, one rich in CuO (L_1) and the other in silver (L_2).

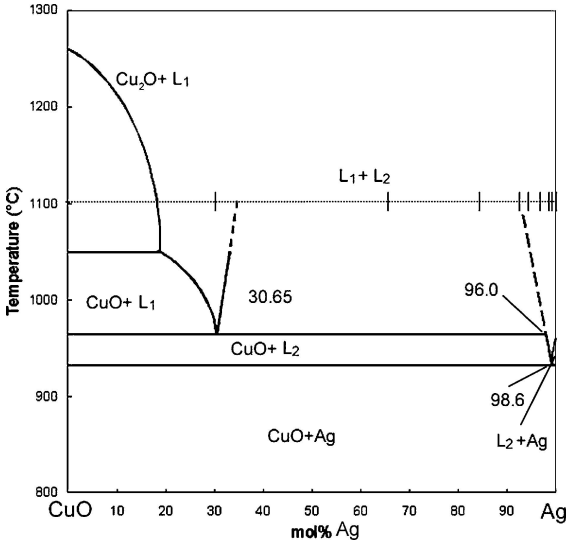

Figure 6 The CuO-Ag phase diagram (from reference [10]). The compositions employed in this study are marked at 1100°C.

Cahn's derivation of critical point wetting predicts a transition in the wetting behavior of a multicomponent liquid in contact with a solid substrate below a critical temperature at which the liquid-liquid immiscibility occurs [14]. Upon reaching this temperature, the previously homogeneous liquid separates into two immiscible liquids. One will perfectly wet the solid substrate and thereby encapsulate the second liquid phase, excluding it from contact with the solid. While Cahn discussed this transition specifically in terms of a critical temperature for a given liquid composition, a similar argument can be applied to define a critical composition at which a wetting transition should be observed when composition is smoothly changed at a given temperature (i.e. as the miscibility gap is entered isothermally). According to Ag-CuO phase diagram, this composition is ∼8 mol% CuO at 1100°C. As the CuO content is increased, we expect that the liquid displaying the lowest interfacial energy with the substrate, presumably the copper oxide-rich L_1 liquid, will preferentially wet the LSCoF substrate to the complete exclusion of the silver-rich L_2 liquid. Thus, a first order transition in contact angle as a function of composition is expected at $x_{CuO} \sim 8$ mol%, which is approximately observed in our data from Fig. 1a.

Unfortunately, a complication arises in our experiments: Cahn's theory assumes an atomistically flat solid substrate, whereas the LSCoF in our experiments contains interconnect surface porosity. So while perfect wetting of the substrate is predicted to occur at the critical point, we do not observe this trend in our wetting results because the L_1 liquid has been drawn into the sub-surface porosity. This implies that it is the behavior of the remaining silver-rich L_2 liquid that defines the wetting angles measured in these sessile drop compositions. Since the concentration of CuO in the L_2 liquid remains the same for both CA16 and CA34, as defined by the tie-line in the two-phase liquid region, the wettability of the CA34 sessile drop should essentially be no different from that of CA16, which corresponds with our finding in Fig. 1a. It is the infiltration data in Fig. 4 that not only independently identifies

a transition point, again at the miscibility gap border of $x_{CuO} \sim 8$ mol%, but also indicates that perfect wetting may occur between the copper oxide-rich L_1 liquid and the LSCoF substrate. Although the data beyond the critical composition is scant, it suggests that the depth of L_1 infiltration increases linearly with CuO content. Under perfect wetting, the entire volume of L_1 in the original molten sessile drop essentially moves into the sub-surface porosity of the substrate under capillary attraction. Since the volume of L_1 is proportional to x_{CuO} (using the tie lines in the phase diagram) and the depth of filled porosity is proportional to the volume of pores (assuming an equivalent volume modeled using a right hand cylinder, $V_{pores} = \pi r^2 d$, where d is the depth of penetration), $x_{CuO} \alpha d$ is predicted when perfect wetting occurs; the same trend observed in our data.

We can also use the Ag-CuO phase diagram to explain our microstructural results. As noted previously, the thermal cycle for these samples ends with a final 15 min soak at 1100°C prior to cooling. Therefore, our analysis begins at this temperature. For example, at 1100°C the eutectic composition (CA01.4) will form a single silver-rich liquid phase on the surface of the LSCoF. Upon cooling to the eutectic temperature, solid Ag and CuO form simultaneously from the eutectic liquid. Driven by the favorable energetics of heterogeneous nucleation, the two phases precipitate preferentially at the LSCoF surface forming a series of finely interspersed Ag and CuO particles. Ideally under a long isothermal hold, the resulting solid should consist of a lath-type morphology commonly observed in slow cooling eutectic alloys [15]. However, the rapid cooling rate appears to have suppressed the formation of this characteristic eutectic microstructure.

In brazes with compositions of 1.4 mol% $< X_{CuO} \lesssim$ 8 mol%, again a single phase liquid forms at 1100°C. However as it cools, a solidus or miscibility composition is reached prior to the eutectic line. For compositions of less than ~4 mol% CuO (the silver-rich end-point of the monotectic line), solid CuO will precipitate out of solution, initially at the LSCoF surface, before any interfacial silver forms; the silver remains in solution as part of the L_2 liquid. For brazes with greater than 4 mol% CuO, the miscibility gap, $L_1 + L_2$, is entered upon cooling. At this point, one of the two liquids is available to wet the LSCoF surface at the exclusion of the other. As proposed earlier, we believe that when segregation takes place between these immiscible liquids, L_1 will preferentially wet the substrate presumably because of its higher CuO content and therefore lower expected interfacial energy with the mixed conducting oxide. Upon further cooling to the monotectic temperature, CuO precipitates out of the L_1 solution along the LSCoF surface. As it does, the silver-rich liquid, L_2, becomes further enriched with silver. In both of the examples above, at the eutectic temperature, solid CuO and Ag simultaneously nucleate from the remaining liquid, presumably in a heterogeneous fashion on the proeutectic CuO and the remaining open LSCoF surface.

As alluded to previously, in the hypomonotectic braze compositions of CA16 and CA34, the sessile drop directly undergoes segregation at 1100°C due to liquid-liquid immiscibility. Again, when the two liquids segregate, the microstructural evidence suggests that the copper oxide-rich liquid preferentially migrates to and wets the LSCoF surface, eventually wicking into the underlying interconnected porosity. For the monotectic composition (CA69), a single phase copper-oxide rich liquid, L_1, forms at 1100°C. As was observed in the micrograph for this specimen, this liquid appears to have rapidly infiltrated the open porosity in the substrate. When cooled to the monotectic temperature, solid CuO and a silver-rich liquid nucleate simultaneously from the silver-poor monotectic liquid. Proportionally, CuO is the major product, accounting for large amount of CuO observed within the LSCoF pores and in the solidified sessile drop. The L_2 liquid likely becomes trapped in the porosity by the surrounding solid CuO and upon further cooling yields the silver deposits observed internally within the substrate.

5. Conclusions

The addition of CuO to silver enhances wetting on $(La_{0.6}Sr_{0.4})(Co_{0.2}Fe_{0.8})O_{3-\delta}$ substrates through a non-reactive mechanism. The largest improvements in contact angle occur at low CuO concentrations via the formation of a homogeneous silver-copper oxide liquid. At a composition of $x_{CuO} \sim 8$ mol%, the wetting mechanism changes as two immiscible liquids form within the sessile drop, each of which can potentially wet the oxide substrate. Based on the metallographic evidence, particularly our observations of a high population of copper oxide deposits within the sub-surface porosity of the substrate, we believe that the copper oxide-rich liquid preferentially wets the LSCoF surface and does so to the exclusion of the silver-rich liquid, following critical point behavior described originally by Cahn.

Acknowledgments

The authors would like to thank Nat Saenz, Shelly Carlson, and Jim Coleman for their assistance in conducting the metallographic and SEM analysis work. This work was supported by the U.S. Department of Energy (U.S. DOE), Office of Fossil Energy, Advanced Research and Technology Development Program. The Pacific Northwest National Laboratory is operated by Battelle Memorial Institute for the U.S. DOE under Contract DE-AC06-76RLO 1830.

References

1. G. R. DOUGHTY and H. HIND, *Key Eng. Mater.* **122–124** (1996) 145.
2. J. W. STEVENSON, T. R. ARMSTRONG, R. D. CARNEIM, L. R. PEDERSON and W. J. WEBER, *J. Electrochem. Soc.* **143** (1996) 2722.
3. Y.-S. CHOU, J. W. STEVENSON, T. R. ARMSTRONG, J. S. HARDY, K. HASINSKA and L. R. PEDERSON, *J. Mater. Res.* **15** (2000) 1505.
4. C. C. SHÜLER, A. STUCK, N. BECK, H. KESER and U. TÄCK, *J. Mater. Sci.: Mater. in Elec.* **11** (2000) 389.
5. K. M. ERSKINE, A. M. MEIER and S. M. PILGRIM, *J. Mater. Sci.* **37** (2002) 1705.

6. K. S. WEIL and D. M. PAXTON, in Proceedings of the 26th Annual Conference on Composites, Advanced Ceramics, Materials, and Structures: A, edited by H.-T. Lin and M. Singh (The American Ceramic Society, Westerville, OH, 2002) p. 263.
7. R. S. ROTH, J. R. DENNIS and H. F. McMURDIE (eds.), "Phase Diagrams for Ceramists" (The American Ceramic Society, Westerville, OH, 1987) Vol. VI, p. 197.
8. A. PETRIC, P. HUANG and F. TIETZ, *Sol. St. Ion.* **135** (2000) 719.
9. D. A. MORTIMER and M. G. NICHOLAS, *J. Mater. Sci.* **8** (1973) 640.
10. Z. B. SHAO, K. R. LIU, L. Q. LIU, H. K. LIU and S. DOU, *J. Am. Ceram. Soc.* **76** (1993) 2663.
11. C. MOURE, D. GUTIERREZ, O. PENA and P. DURAN, *J. Sol. St. Chem.* **163** (2002) 377.
12. H. W. HSU, Y. H. CHANG, G. J. CHEN and K. J. LIN, *Mater. Sci. and Eng. B* **B64** (1999) 180.
13. R. S. ROTH, J. R. DENNIS and H. F. McMURDIE (eds.), "Phase Diagrams for Ceramists" (The American Ceramic Society, Westerville, OH, 1987), Vol. V, p. 345.
14. J. W. CAHN, *J. Chem. Phys.* **66** (1977) 3667.
15. R. N. GRUGEL and A. HELLAWELL, *Met. Trans.* **12A** (1981) 669.

Received 31 March
and accepted 18 July 2004